Tunable Surface Plasmon Band of Position Selective Ag and Au Nanoparticles in Thin Block Copolymer Micelle Films

ARTICLE *in* CHEMISTRY OF MATERIALS · AUGUST 2009

Impact Factor: 8.35 · DOI: 10.1021/cm901245g

6 AUTHORS, INCLUDING:

Dong Ha Kim
Ewha Womans University
136 PUBLICATIONS **3,100** CITATIONS

SEE PROFILE

Cheolmin Park
Yonsei University
127 PUBLICATIONS **4,129** CITATIONS

SEE PROFILE

4248 *Chem. Mater.* **2009,** *21,* 4248–4255
DOI:10.1021/cm901245g

CHEMISTRY OF MATERIALS
Article

Tunable Surface Plasmon Band of Position Selective Ag and Au Nanoparticles in Thin Block Copolymer Micelle Films

Himadri Acharya,[†] Jinwoo Sung,[†] Byeong-Hyeok Sohn,[‡] Dong Ha Kim,[§] Kaoru Tamada,[⊥] and Cheolmin Park*,[†]

[†]*Department of Materials Science and Engineering, Yonsei University, Seoul 120-749, Korea,* [‡]*Department of Chemistry, Seoul National University, Seoul, Korea,* [§]*Division of Nano Sciences and Department of Chemistry, Ewha Womans University, 11-1 Daehyun-Dong, Seodaemun-Gu, Seoul 120-750, Korea, and* [⊥]*Research Institute of Electrical Communication, Tohoku University, 2-1-1 Katahira, Aoba-ku, Sendai 980-8577, Japan*

Received May 5, 2009. Revised Manuscript Received July 14, 2009

The manuscript describes a novel method to fabricate a thin composite film based on spin coating in which surface plasmon bands of Au and Ag nanoparticles are effectively coupled with each other because of position-selective deposition of both nanoparticles on a self-assembled block copolymer structure. Simple solution blending and subsequent spin coating of Au nanoparticles (NPs) and a block copolymer micelles containing Ag NPs in the core regions offers a facile route for controlling coupled surface plasmon band (SPB) of the two NPs over 100 nm in wavelength in thin solid films. Effective coupling of two individual SPBs relies upon the self-assembled composite structure where Ag and Au NPs are preferentially located in the core and corona regions of the micelles, respectively, allowing not only a controlled interparticle distance but also homogeneous dispersion of the NPs throughout film.

Introduction

The plasmonic coupling between metal NPs is one of the most intriguing optical properties, and its characteristic enhancement of local optical field at particle−particle junction is enormously useful for many sensing applications.[1−4] The synergistic control of various key parameters sensitive to the surface plasmon band (SPB) even broadens its potentials and at the same time allows us to tune the SPB, including particle size and shape, surrounding dielectric medium, interparticle distance, and their structural position.[5−8]

Further control of SPB in wider range has been achieved by bimetallic nanoparticles fabricated in the form of either core−shell or alloy of two metals. The interaction of the two metallic components in either nanometer or atomic scale permits facile tuning of SPB mostly in solution phases. The resulting SPB in general lies in between that of the pure component, depending on the relative amounts of the two components.[9−12] For example, SPB maxima of Au/Ag alloy nanoparticles either blue-shifted or red-shifted linearly with an increase in Ag or Au content, respectively.[13,14] The absorbance properties of Ag and Au core−shell particles generally depend on the shell thickness and dielectric environment.[15,16] The Au plasmon band of Au core−Ag shell nanoparticles shifted to the lower wavelength with an increase in Ag shell thickness.[17,18] Interestingly, the case of the Ag core−Au shell bimetallic nanoparticle prepared either in beta cyclodextrine (β-CD)[18] or by laser ablation[19] shows a single SPB tuned over the entire wavelength region of pure Ag and Au. This phenomenon of SPB peak shift with shell thickness was also further investigated using simulation of absorption spectra based on Mie theory.[19−21] The SPB coupling between individual nanoparticles was also

*Corresponding author. Tel: 82-2-2123-2833. Fax: 82-2-312-5375. E-mail: cmpark@yonsei.ac.kr.

(1) Stewart, M. E.; Anderton, C. R.; Thompson, L. B.; Maria, J.; Gray, S. K.; Rogers, J. A.; Nuzzo, R. G. *Chem. Rev.* **2008**, *108*, 494.
(2) Lee, J.-S.; Han, M. S.; Mirkin, C. A. *Angew. Chem., Int. Ed.* **2007**, *46*, 4093.
(3) Gao, D.; Chen, W.; Mulchandani, A.; Schultz, J. S. *Appl. Phys. Lett.* **2007**, *90*, 073901/1.
(4) Liu, J.; Lu, Y. *Angew. Chem., Int. Ed.* **2006**, *45*, 90.
(5) Liz-Marzaran, L. M. *Langmuir* **2006**, *22*, 34.
(6) Chen, H. M.; Hsin, C. F.; Liu, R.-S.; Lee, J.-F.; Jang, L.-Y. *J. Phys. Chem. C* **2007**, *111*, 5909.
(7) Lee, K.-S.; El-Sayed, M. A. *J. Phys. Chem. B* **2006**, *110*, 19220.
(8) Murphy, C. J.; Sau, T. K.; Gole, A.; Orendorff, C. J. *MRS Bull.* **2005**, *30*, 349.
(9) Anandan, S.; Grieser, F.; Ashokkumar, M. *J. Phys. Chem. C* **2008**, *112*, 15102.
(10) Xu, Z.; Hou, Y.; Sun, S. *J. Am. Chem. Soc.* **2007**, *129*, 8698.
(11) Kalsin, A. M.; Fialkowski, M.; Paszewski, M.; Smoukov, S. K.; Bishop, K. J. M.; Grzybowski, B. A. *Science* **2006**, *312*, 420.
(12) Mandal, S.; Selvakannan, P. R.; Pasricha, R.; Sastry, M. *J. Am. Chem. Soc.* **2003**, *125*, 8440.
(13) Link, S.; Wang, Z. L.; El-Sayed, M. A. *J. Phys. Chem. B* **1999**, *103*, 3529.
(14) Mallin, M. P.; Murphy, C. J. *Nano Lett.* **2002**, *2*, 1235.
(15) Cao, Y. W.; Jin, R.; Mirkin, C. A. *J. Am. Chem. Soc.* **2001**, *123*, 7961.
(16) Xu, S.; Zhao, B.; Xu, W.; Fan, Y. *Colloids Surf., A* **2005**, *257−258*, 313.
(17) Lim, D. K.; Kim, I. J.; Nam, J. M. *Chem. Commun.* **2008**, 5312.
(18) Pande, S.; Ghosh, S. K.; Praharaj, S.; Panigrahi, S.; Basu, S.; Jana, S.; Pal, A.; Tsukuda, T.; Pal, T. *J. Phys. Chem. C* **2007**, *111*, 10806.
(19) Han, H.; Fang, Y.; Li, Z.; Xu, H. *Appl. Phys. Lett.* **2008**, *92*, 023116.
(20) Wang, X.; Zhang, Z.; Hartland, G. V. *J. Phys. Chem. B* **2004**, *108*, 5882–5888.
(21) Moskovits, M.; Srnová-loufová, I; Vlková, B. *J. Chem. Phys.* **2002**, *116*, 10435.

 Published on Web 08/17/2009

achieved in the systems where the interparticle distance and dielectric properties were carefully controlled during either self-assembly[22,23] or reconfiguration[24] of molecular linkers attached on the surface of the nanoparticles. The recent work by Sebba et al. has demonstrated that for example SPB of Au and Ag nanoparticles is controlled when Au (Ag) satellite particles are linked to the Au (Ag) cores mediated by reconfigurable DNA strands.[25]

For more broad utilization of the tunable plasmon frequency in particular in thin solid films, one should consider two important aspects in our opinion. First of all, the relative amount of two metallic components need to be more easily controlled than in the core−shell or alloyed nanoparticles, which requires somewhat a time-consuming process for varying the composition of two components. One of the most practical ways would be the blending of two metal NPs, but the constant interparticle distance for coherent surface plasmonic coupling is rarely obtained because of the characteristic macroscopic aggregates of each component in blend films. Second, nanoparticles should be distributed homogeneously throughout a thin film with the constant nanometer scale interparticle distance for plasmon coupling.

Self-organizing BCP micelles[26−28] capable of locating metal NPs selectively in their cores and coronas provides an interesting platform in which position dependent surface plasmons of metal NPs can be examined in thin films. One expects that interparticle distance between two different metal NPs located in corona and core, respectively, can be easily controlled by the chain length of the component blocks. In addition, BCP micelles with the site selective nanoparticles may prohibit the possible macroscopic aggregates, leading to the mixture of nanoparticles homogeneously dispersed throughout a thin composite film.

In this contribution, we fabricate thin a poly(styrene-*b*-4vinyl pyridine) (PS-*b*-P4 VP) copolymer micelle film with position controlled Ag and Au NPs selectively located in the cores and coronas of the micelles, respectively. The controlled interparticle distance of Ag and Au NPs in a BCP film gave rise to a broad tunability of the coupled plasmon frequency of the two nanoparticles ranging from 450 to 550 nm as a function of relative amount of Au and Ag NPs.

Experimental Section

Materials. Three poly(styrene-*block*-4vinyl pyridine) (PS-*b*-P4 VP) copolymers, PS-*b*-P4 VP (19K/22K, 19 000−22 000 g/mol), PS-*b*-P4 VP (47K/21K, 47 600−20 900 g/mol) and PS-*b*-P4 VP (122K/22K, 122 000−22 000 g/mol) were purchased from Polymer Source Inc. Doval, Canada. The polydispersity indexes (PDI) of the copolymers are 1.15, 1.14, and 1.15, respectively. Silver acetate, auric acid ($HAuCl_4$,$3H_2O$), tertraoctylammonium bromide ($(C_8H_{17})_4NBr$), and sodium borohydride ($NaBH_4$) were purchased from Aldrich, Korea.

Dodecanethiol Protected Au Nanoparticles. The dodecane thiol ($C_{12}H_{25}SH$) (DT) modified Au nanoparticles (DT-Au NPs) were synthesized by a two-phase Brust's reduction method.[29] Gold-ion aqueous solution ($HAuCl_4 \cdot 3H_2O$) was mixed with tertraoctylammonium bromide ($(C_8H_{17})4NBr$), a phase transfer catalyst (PTC) in toluene. Subsequently, DT and an aqueous sodium borohydride ($NaBH_4$) were added as surface protection group and reducing agent, respectively, and stirred overnight. Nanoparticles in toluene phase were separated in a rotary evaporator, and purified by successive washing in ethanol several times to remove the phase transfer catalyst, excess DT, and reaction byproducts. The product was redispersed in toluene and size-selective nanoparticles were precipitated using ethanol as nonsolvent during centrifugation.

Nanocomposites of PS-*b*-P4 VP/Ag/Au. A PS-*b*-P4 VP solution in toluene with a concentration of 1 wt % was prepared. The polar P4 VP block of PS-*b*-P4 VP copolymer is insoluble in toluene and forms spherical micelle with P4 VP core and soluble PS corona. AgAc (Aldrich) (molar ratio of silver acetate/vinylpyridine = 0.3) was first added and sonicated with a power of 80 W, a frequency of 40 kHz to coordinate within P4 VP core of micelle. We utilized the sonication just to disperse AgAc effectively in the solution. The selective coordination of AgAc in the P4 VP core regions occurs because of the specific interaction between AgAc and pyridine groups, which donate lone pair electrons of nitrogen atoms to Ag ions of AgAc. It is well-known that a variety of metal salts or precursors of metal nanoparticles can be selectively coordinated to the P4 VP core of block copolymer micelle.[30,31] The solution is colorless and does not show any characteristic Ag absorbance peak (Supporting Information, Figure S1). A desired amount of DT-Au NPs, previously synthesized, was added and sonicated for complete dispersion. The amount of Au nanoparticle relative to the polymer was varied from 0.5 to 100 wt %. Thin nanocomposite films were prepared by spin coating the block copolymer solution containing DT-Au NPs and AgAc on glass substrate at 2000 rpm for 60 s. The glass substrates prior to film preparation were cleaned by treating with 25% NH_4OH/35% H_2O_2 ((2/1) (v/v)) for 1 h and then washed with deionized water. The nanocomposite films were dried at room temperature in a vacuum for 12 h in order to remove the residual solvent completely. The reducing agent free synthesis of Ag nanoparticles was carried out by a method similar to one developed by J. Zhang et al.[32] In our case, thermal annealing at 200 °C for 12 h was sufficient to reduce AgAc into a few of Ag nanoparticles in a core with the diameter of approximately 5 nm. The selective loading of Ag and Au NPs in the core and corona regimes of a PS-*b*-P4 VP copolymer, respectively, is depicted in the schematic of Figure 1.

Characterization. UV−vis measurements for surface plasmon resonance absorbance were carried out with a JASCO V-530

(22) Mirkin, C. A.; Letsinger, R. L.; Mucic, R. C; Storhoff, J. J. *Nature* **1996**, *382*, 607.
(23) Alivisatos, A. P.; Johnsson, K. P.; Peng, X. G.; Wilson, T. E.; Loweth, C. J.; Bruchez, M. P; Schultz, P. G. *Nature* **1996**, *382*, 609.
(24) Sonnichsen, C.; Reinhard, B. M.; Liphard, J.; Alivisatos, A. P. *Nat. Biotechnol.* **2005**, *23*, 741.
(25) Sebba, D. S.; LaBean, T. H.; Lazarides, A. A. *Appl. Phys. B: Laser Opt.* **2008**, *93*, 1803.
(26) Sung, J.; Jo, P. S.; Shin, H.; Huh, J.; Min, B. G.; Kim, D. H.; Park, C. *Adv. Mater.* **2008**, *20*, 1505.
(27) Hwang, W.; Choi, J.-H.; Kim, T. H.; Sung, J.; Myoung, J.-M.; Choi, D.-G.; Sohn, B.-H.; Lee, S. S.; Kim, D. H.; Park, C. *Chem. Mater.* **2008**, *20*, 6041.
(28) Sohn, B. H.; Choi, J. M.; Yoo, S. I.; Yun, S. H.; Zin, W. C.; Jung, J. C.; Kanehara, M.; Hirata, T.; Teranishi, T. *J. Am. Chem. Soc.* **2003**, *125*, 6368.
(29) Brust, M.; Walker, M.; Bethell, D.; Schiffrin, D. J.; Whyman, R. *J. Chem Soc., Chem Commun.* **1995**, 1655.
(30) Bronstein, L.; Antonietti, M.; Valetsky, P. In *Nanoparticles and Nanostructured Films*; Fendler, J. H., Ed.; Wiley-VCH: Weinheim, Germany, 1998.
(31) Hamley, I. W. *Nanotechnology* **2003**, *14*, R39.
(32) Zhang, J.; Gao, Y.; Alvarez-Puebla, R. A.; Buriak, J. M.; Fenniri, H. *Adv. Mater.* **2006**, *18*, 3233.

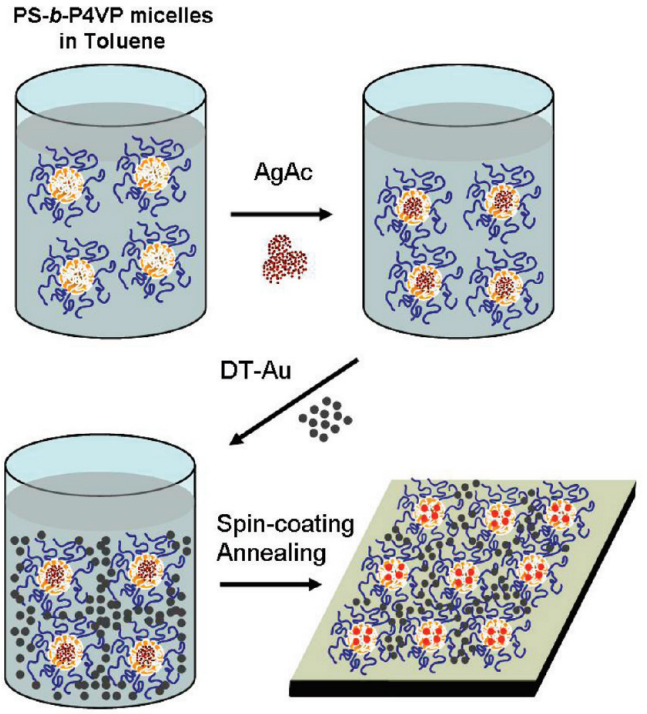

Figure 1. Schematic illustration of fabrication of the block copolymer/Ag/Au nanoparticles composite films. A thin transparent composite film is prepared with site-selective Ag and Au NPs preferentially located in the core and corona regions of block copolymer micelles, respectively, by spin coating, followed by thermal annealing at 200 °C for 12 h.

UV−vis spectrophotometer. All measurements of nanocomposite thin film were performed in air. A baseline correction procedure was executed prior to each measurement session. The scan speed was 200 nm min^{-1}. To prepare the samples for transmission electron microscopy (TEM), we spin-coated a PS-*b*-P4 VP block copolymer solution on a carbon-coated copper grid and dried it in a vacuum at 50 °C for 24 h. The samples were subsequently annealed. Electron microscope images were recorded on a TEM, Hitachi H-600 and HRTEM, Jeol 2100 operated at 50 and 200 kV in bright field, respectively. X-ray Photoelectron Spectra (XPS) were measured with SIGMA PROBE (ThermoVG, UK) at room temperature using a monochromatic Al Kα X-ray source at 12 kV and 100 W. The sample analysis chamber of the XPS instrument was maintained at a pressure of 1.8×10^{-9} mb. All the spectra were fitted with nonlinear least-squares fitting using both XPS peak fitting software and Shirley background consideration.

Results and Discussion

The coupled SPB of Ag and Au NPs is controlled by incorporating the nanoparticles selectively into core and corona regions of a thin film of PS-*b*-P4 VP micelles as shown in the schematic of Figure 1. The polar P4 VP block of PS-*b*-P4 VP copolymer becomes insoluble in toluene and consequently forms spherical micelle with P4 VP core and soluble PS corona. A metallic salt, silver acetate (AgAc) was preferentially loaded in the P4 VP core regions in solution. The reduction of AgAc to Ag nanoparticles can be possible during sonication process in which the radicals generated by acoustic cavitation may reduce the metal salt to metal nanoparticles. The ultrasound frequency generates acoustic cavitation in the solution where the gas bubbles during cavitation impart local heating which subsequently induces a vibrational motion to the molecules resulting in reducing metal salts into nanoparticles. This method of sonochemical dispersions has been also reported elsewhere.[33,34] In our system, however, we did not observe Ag NPs formation during sonication process. A PS-*b*-P4 VP(47K/21K) film with AgAc by sonication dispersion shows no characteristic SPB from Ag NPs (Supporting Information, Figure S1).

To selectively locate Au NPs in the corona regions of the micelles, we added Au NPs to the solution that had been synthesized by a solvent exchange method and subsequently thermally annealed at 150 °C.[35] Figure 2a shows DT-Au NPs deposited on a carbon-coated grid surface with the average particle size of approximately 5−6 nm in diameter. A HRTEM image in the inset also exhibits that Au nanoparticlesg are highly crystalline. Spin-coating of the composite solution, followed by thermal annealing at 200 °C for 12 h, allowed us to prepare a thin, transparent, and uniform film on a glass substrate.

The position-selective incorporation of Ag and DT-Au NPs in a thin PS-*b*-P4 VP(47K/21K) micelle film was independently revealed by bright-field TEM as shown in images b and c in Figure 2, respectively. The thermal annealing effectively reduced the AgAc into Ag NPs with the diameter of approximately 5 nm in the cores as shown in Figure 2b. Depending upon the reduction condition, both size and its distribution of Ag nanoparticles are varied over a wide range as demonstrated for Au nanoparticles. The interaction between Ag ion and P4 VP block reduces the ion mobility and thus allows the free metal ions to nucleate and grow to Ag NPs. The fast self-assembly of the micelles during spin-coating first gave rise to closed-packed micelle arrays with a pseudo hexagonal symmetry. DT-Au NPs dispersed with the micelles are preferentially sequestered from the highly swollen and entangled corona PS blocks because of entropic penalty and thus tend to find their position selectively in the intermicelle regions of the hexagonally packed micelles during spin coating as shown in Figure 2c. It is noted that 1 wt % block copolymer solution used is sufficiently concentrated to form a pseudo closed packing of highly swollen BCP micelles even in solution, rendering DT-Au NPs preferentially located at the regions between two micelles as schematically depicted in Figure 1. The closed packing of the micelles was confirmed by the characteristic reflection around 390 nm in UV−vis spectroscope in solution (Supporting Information, S2).

The representative microstructure of a thin PS-*b*-P4 VP(47K/21K) film with the position selected both Ag NPs and DT-Au were revealed by bright-field TEM as shown in Figure 3a. Because of the difference in electron density of the two nanoparticles, it is difficult to simultaneously visualize both Ag and DT-Au NPs in TEM. The

(33) Flint, E. B; Suslick, K. S. *Science* **1991**, *253*, 1397.
(34) Le, L. Y; Sacchi, L. H. *Ultrason. Symp.* **2004**, *1*, 565–568.
(35) Teranishi, T.; Hasegawa, S.; Shimizu, T.; Miyake, M. *Adv. Mater.* **2003**, *13*, 1699.

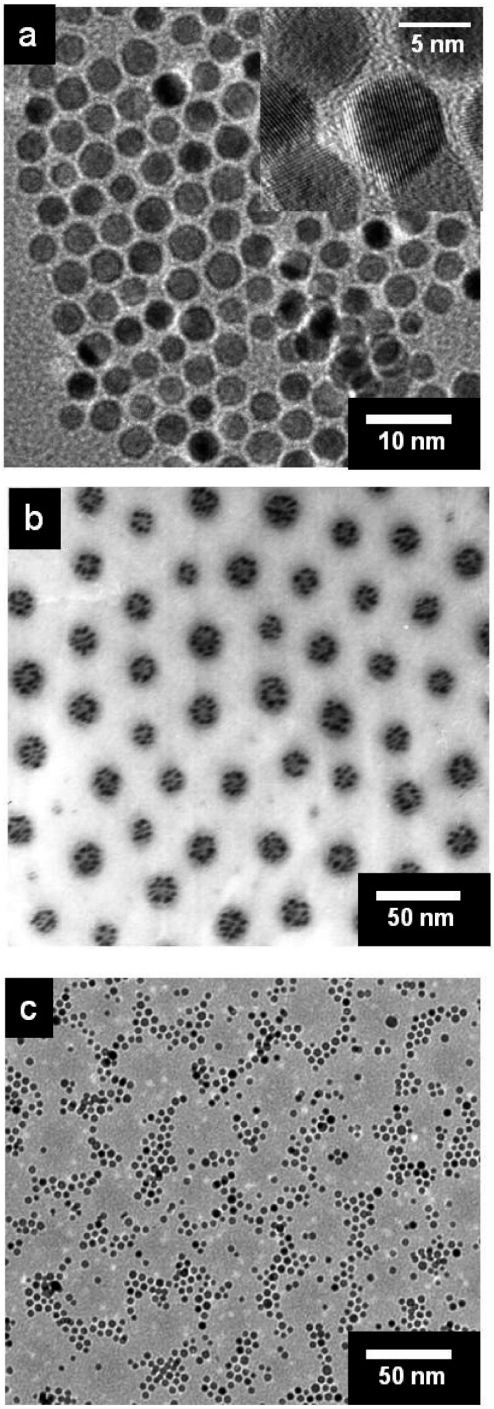

Figure 2. Bright-field TEM image of (a) dodecanethiol protected Au nanoparticles. A HRTEM image in the inset shows Au nanoparticles with high crystalline order. Bright field TEM micrographs of (b) an Ag NPs/PS-*b*-P4 VP(47K/21K) composite film in which Ag NPs are preferentially formed in the core regions of the micelles by thermal annealing and (c) a DT-Au NPs/PS-*b*-P4 VP(47K/21K) composite film in which DT-Au NPs are preferentially located in the corona regions of the micelles.

assembled DT-Au NPs in the outer corona regions are apparent on focus while somewhat diffused cores are observed in which Ag NPs are supposed to be located in Figure 3a. Ag NPs in the cores are clearly visible with different focal length in TEM as shown in the inset of Figure 3a. The coexistence of DT-Au and Ag NPs in the composite film was also confirmed by Energy Dispersive X-ray spectroscopy (EDX) analysis in Figure 3a. The

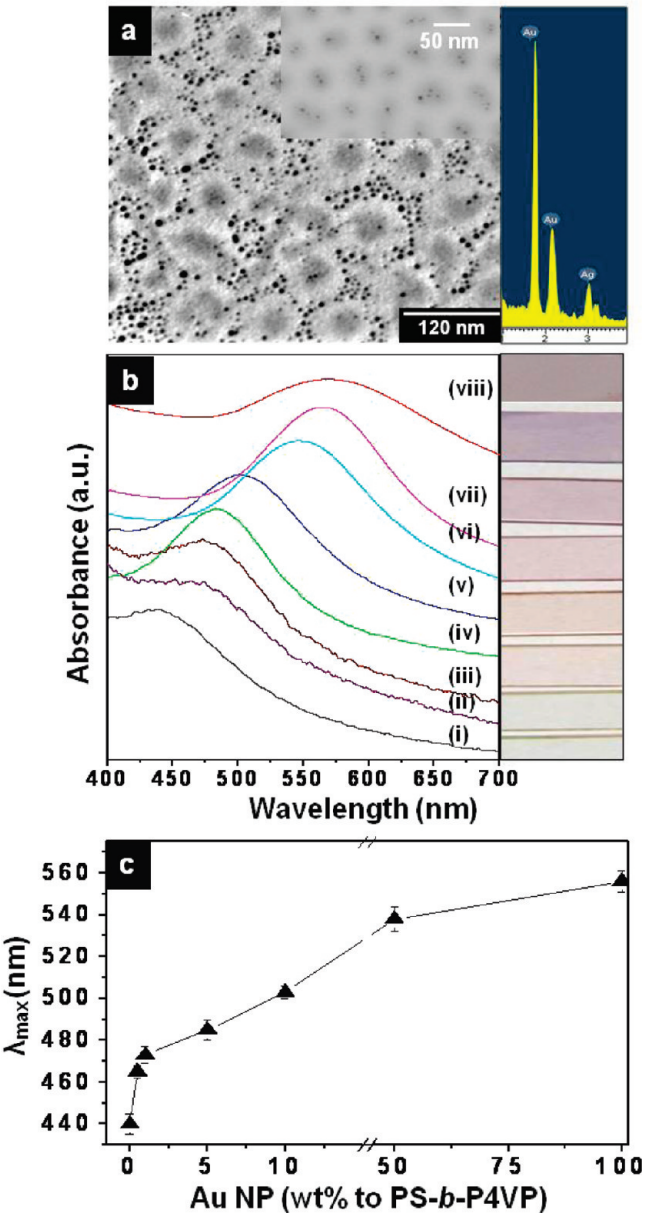

Figure 3. (a) Bright-field TEM micrograph of a thin PS-*b*-P4 VP(47K/21K)/Ag/DT-Au NPs composite film spin coated and annealed at 200 °C for 12 h. The weight fraction of DT-Au NPs is 0.1 with respect to the block copolymer in the composite. DT-Au NPs are apparent on focus, preferentially located in the intermicelle regions of the micelles pseudohexagonally packed. Ag NPs are visible in different focal length in the inset. An EDX spectrum shown on the right-hand side clearly indicates the coexistence of Au and Ag NPs in the composite film. (b) UV−vis absorbance spectra of a series of PS-*b*-P4 VP(47K/21K)/Ag/DT-Au NPs composite films as a function of amount of DT-Au NPs ranging from 0 to 100 wt % with respect to the block copolymer. The amount of Ag NPs is fixed in all the composites with the AgAc concentration of 0.3 equiv. with respect to P4 VP blocks. Au concentration changes in the range of (i) 0, (ii) 0.5, (iii) 1, (iv) 5, (v) 10, (vi) 50, and (vii) 100 wt % with respect to block copolymer. For comparison, a spectrum of a composite only with 100 wt % DT-Au NPs is shown in (viii). A photograph of the samples examined with UV−vis spectrometer clearly shows the red-shift of film color with DT-Au NPs in the composites. (c) A plot of the surface plasmon absorbance maxima of (b) as a function of DT-Au NPs.

characteristic X-ray peaks are observed at 1.78 and 2.19 for Au and 3.1 eV for Ag, respectively. Our results imply that the thermal annealing at 200 °C is effective for reducing AgAc to Ag NPs without possible interparticle sintering with DT-Au NPs in the films.

Figure 3b shows UV−vis absorbance results of a series of thin PS-*b*-P4 VP(47K/21K) /Ag/DT-Au NPs films with different amount of DT-Au NPs. BCP films only with either Ag or DT-Au NPs correspond to (i) and (viii) in Figure 2b, respectively and exhibit the characteristic absorbance peaks around 442 and 556 nm, arising from surface plasmon resonance of Ag NPs and DT-Au NPs with approximately 5 nm and 5−6 nm in diameter, respectively.[36,37] The variation of the relative amount of two nanoparticles in a BCP film enabled us to control the characteristic surface plasmon frequency arising from effective coupling of two individual peaks as shown in (ii) to (vii) of Figure 3b. It is obvious that the peak position is shifted to red with the amount of Au NPs in a film. A photograph in Figure 3b also clearly exhibits color change with DT-Au NPs in the composites. A plot of the maximum peak positions as a function of the amount of DT-Au NPs displays the modulation of the coupled SPB as shown in Figure 3c.

We also investigated UV−vis spectra of PS-*b*-P4 VP-(47K/21K) films with DT-Au NPs and AgAc preferentially in the corona and core regions, respectively, before thermal annealing for the reduction of AgAc to Ag NPs. Spectra (i), (ii), and (iii) in Figure 4a show SPB at approximately 534 nm arising from the resonance of pure DT Au NPs when DT-Au NPs are added up to 10 wt % with respect to the block copolymer. Thermal annealing of the samples clearly developed three coupled SPB at the different wavelengths of approximately 466, 482, and 502 nm, which correspond to (iv), (v), and (vi) in Figure 4a, respectively. The results imply that Ag NPs reduced by the thermal annealing are effectively interacted with DT-Au NPs in SPB, consistent with our results in Figure 3b.

There is a concern that Au SPB may be affected by AgAc physically absorbed in the corona regions during hybridization due to the considerable change in dielectric property of the surrounding media. First of all, in order to examine the effect of AgAc physically absorbed in the corona regions on Au SPB, we mimicked the situation with PS homopolymer in which excess AgAc remaining after the preferential loading in the P4 VP cores may be physically deposited in the PS corona regions in the block copolymer micelles. We prepared composite films with PS homopolymer spin coated and thermally annealed from two different solutions: one with DT-Au NPs and the other with both DT-Au NPs and AgAc. Both films show no difference in SPB of Au NPs as shown in Figure 4b, which indicates either that AgAc was not physically absorbed on DT-Au NPs or that even if it is physically absorbed in the PS regions, AgAc does not significantly influence the Au SPB. For further confirmation, we also prepared the PS-*b*-P4 VP(47K/21K) films with 10 wt % DT-Au NPs with respect to the copolymer containing the different amount of AgAc. UV−vis spectra of the samples in Figure 4c also exhibit no significant alteration of SPB at approximately 534 nm, which indicates that the presence of AgAc in the block copolymer micelles does not affect Au SPB by changing the dielectric property of the medium.

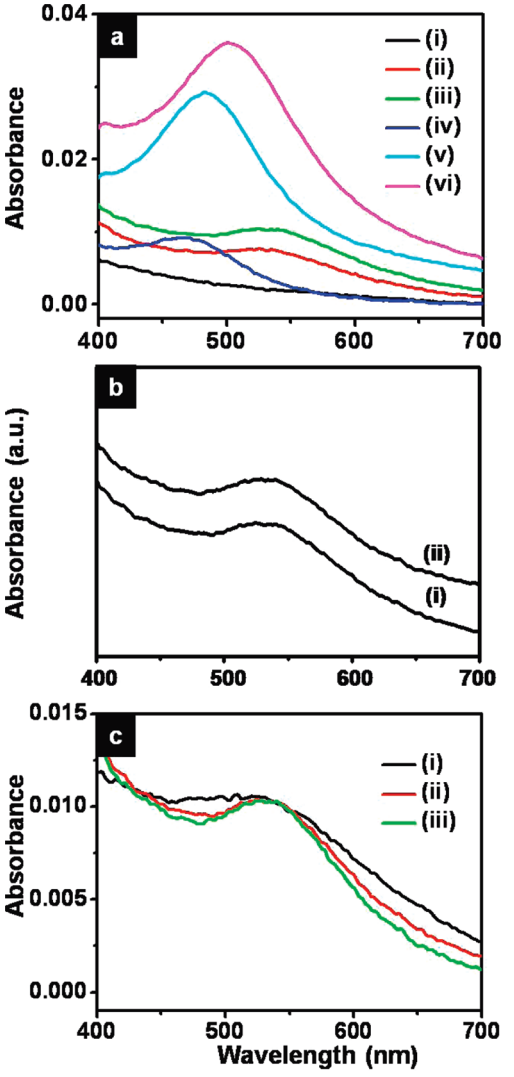

Figure 4. (a) UV−vis absorbance spectra of PS-*b*-P4 VP(47K/21K) films with AgAc and DT-Au NPs preferentially in the core and corona regions, respectively, (i, ii, iii) before and (iv, v, vi) after thermal annealing. The amount of AgAc is fixed (0.3 equiv with respect to P4 VP), whereas DT-Au NPs increases from (i) 1, (ii) 5, and (iii) 10 wt %. SPB peaks at approximately 534 nm, arising from the resonance of DT Au NPs, which does not shift significantly with Au concentration. After thermal annealing, the coupled SPB between the reduced Ag NPs and DT-Au NP is gradually shifted to 466, 482, and 502 nm with the DT-Au NP of (iv) 1, (v) 5, and (vi) 10 wt %, respectively. (b) UV−vis absorbance spectra of thin PS homopolymer films spin-coated and thermally annealed from two different solutions: (i) with DT-Au NPs and (ii) with both DT-Au NPs and AgAc. The SPB peak at 534 nm of Au NPs (10 wt % with respect to PS homopolymer) does not change. (c) UV−vis spectra of PS-*b*-P4 VP(47K/21K)/Ag/DT-Au NPs composite films with three different amounts of AgAc of (i) 0, (ii) 0.3, and (ii) 1 equivalent with respect to P4 VP block before thermal annealing. The amount of DT-Au NPs is fixed as 10 wt % with respect to copolymer. The presence of AgAc in the block copolymer micelles does not affect Au SPB peak at approximately 534 nm by changing the dielectric property of the medium.

Our UV−vis results in Figure 3 are very similar to those previously observed in either core−shell type Ag−Au nanoparticles or bimetallic alloyed particles of Au and Ag in solution. This clearly indicates that simple blending

(36) Logar, M.; Jancar, B.; Suvorov, D.; Kostanjsek, R. *Nanotechnology* **2007**, *18*, 325601.
(37) Daniel, M.-C.; Astruc, D. *Chem. Rev.* **2004**, *104*, 293.

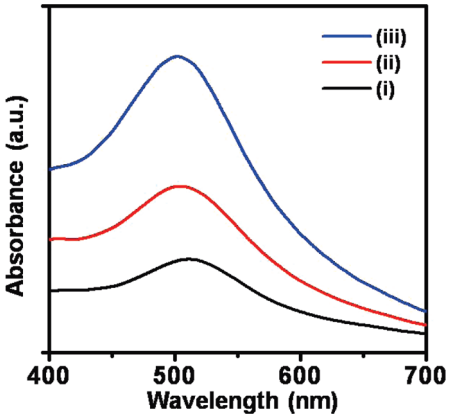

Figure 5. UV−vis absorbance of position selective bimetallic nanoparticles in PS-*b*-P4 VP(47K/21K) by varying the film thickness using different solution concentration from (i) 0.5, (ii) 1, and (iii) 2 wt % in toluene. The amount of Ag NPs and DT-Au NPs is fixed as 0.3 equiv to P4 VP block and 10 wt % with respect to copolymer, respectively.

of two nanoparticles is also useful for tuning the coupled SPB, combined with BCP nanostructure capable of defining the position of each nanoparticle in thin films. The SPB is strongly correlated with particle size, interparticle distance, and dielectric medium properties, and Mie theory has well-described the resonance behavior as a simple model.[38] In our system, both particle size and interparticle distance are presumably that same as DT-Au and Ag NPs in a composite film in spite of a small variation of the interparticle distance arising from the spacial distribution of Au NPs in the corona regions. In addition, a regularly arrayed structure with relatively longer distance (~100 nm or more) with metallic objects has been known to excite surface dipole field similar to the propagating surface plasmons. The shift and broadening of the plasmon resonance are essentially determined by the periodicity of the array. The dipole fields of neighboring particles are superimposed with their respective phase shift, which depends on the distance between the particles. In our system, we also expect that a similar surface dipole field that arises from Au and Ag nanoparticles regularly positioned in the periodic block copolymer micelle structure plays an additional role for the tunable SPB band of the two nanoparticles. This type of long-range dipolar interaction between the two nanoparticles over the distance greater than approximately 15 nm has been evidenced both experimentally and theoretically in the previous studies.[39−42] The absolute absorption intensity of a composite film almost linearly increases at the maximum peak position with the concentration of block copolymer, indicative of the long-range dipolar coupling between Ag and Au NPs as shown in Figure 5.

We also examined the effect of nanoparticle aggregation on SPB shift by varying the amount of DT-Au NPs in a PS-*b*-P4 VP(47K/21K) film without Ag NPs. There is no significant SPB red-shift observed in the film when DT-Au NPs was loaded up to 20 wt % with respect to the block copolymer (see the Supporting Information, Figure S3). Considering that more than 60 nm SPB peak shift in wavelength was detected with 20 wt % DT-Au NPs in the presence of Ag NPs in Figure 3b, the aggregation effect on SPB in our system can be negligible. It should be noted that SPB of DT-Au NPs was shifted from approximately 534 to 556 nm when loaded more than 100 wt % with respect to the block copolymer, which implies that there still exists some aggregation effect on SPB at heavily loaded samples.

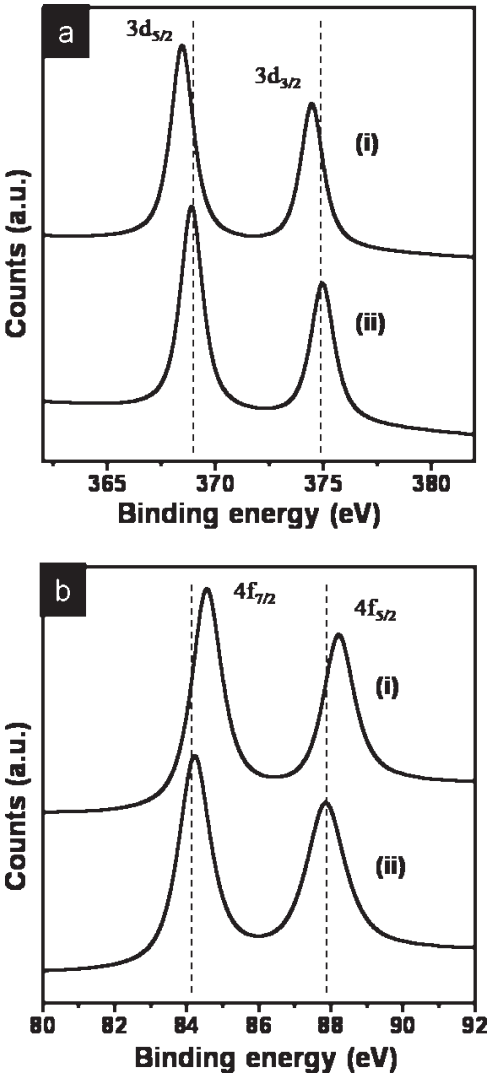

Figure 6. (a) XPS spectra of Ag NPs preferentially located in the core regions of a PS-*b*-P4 VP(47K/21K) micelle film (i) with and (ii) without DT-Au NPs in the corona regions. (b) XPS spectra of Au NPs preferentially formed in the corona regions of a PS-*b*-P4 VP(47K/21K) micelle film (i) with and (ii) without Ag NPs in the core regions.

The SPB coupling between Ag and Au NPs preferentially located in the block copolymer film was further evidenced by XPS analysis in Figure 6. Figure 6a shows XPS spectra of Ag NPs preferentially loaded in the cores of PS-*b*-P4 VP(47K/21K) micelles with or without DT-Au NPs. Both spectra clearly exhibit the characteristic $3d_{5/2}$ and $3d_{3/2}$ spin orbit components of Ag NPs. When DT-Au NPs were incorporated selectively in the corona

(38) Mie, G. *Ann. Phys.* **1908**, *25*, 377.
(39) Lamprecht, B.; Schider, G.; Lechner, R. T.; Ditlbacher, H.; Kren, J. R.; Leitner, A.; Aussenegg, F. R. *Phys. Rev. Lett.* **2000**, *84*, 4721.
(40) Meier, M.; Wokaun, A.; Liao, P. F. *J. Opt. Soc. Am. B* **1985**, *2*, 931.
(41) Papanikolaou, N. *Phys. Rev. B* **2007**, *75*, 235426.
(42) Ghoshal, A; Kik, P. G. *J. Appl. Phys.* **2008**, *103*, 113111.

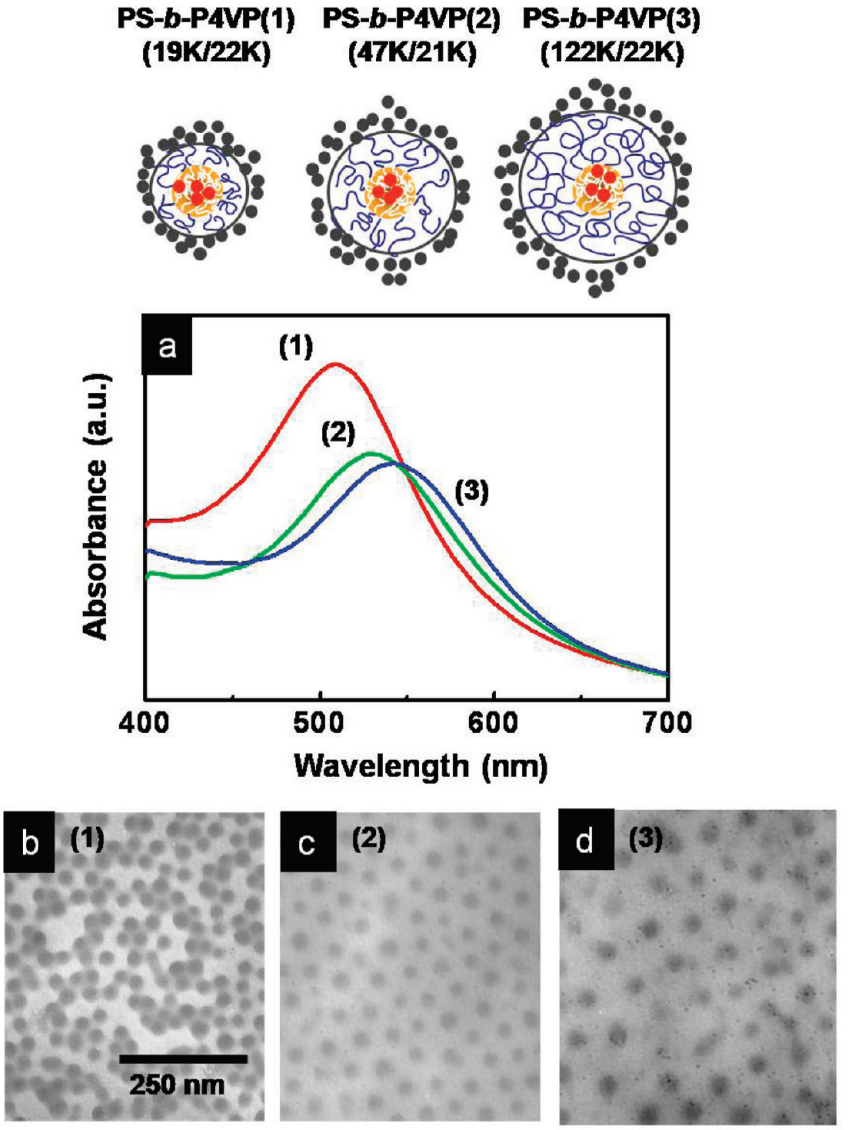

Figure 7. UV−vis absorbance spectra of PS-*b*-P4 VP/Ag/DT-Au NPs composite films with 3 different PS-*b*-P4 VP copolymers: (19K/22K), (47K/21K) and (122K/22K) of the molecular weights of PS/P4 VP. The amount of DT-Au NPs is fixed as 20 wt % with respect to copolymer. The absorbance maxima tend to be red-shifted with an increase in the molecular weight of PS block because of the increase in interparticle distance between Ag and DT-Au NPs in the films. A schematic in the figure represents variation in the interparticle distance between Ag and DT Au NPs due to the change in the molecular weights of PS blocks in the three different block copolymers. Bright-field TEM micrographs of monolayered micelles of (b) PS-*b*-P4 VP(19K/22K), (c) PS-*b*-P4 VP(47K/21K), and (d) PS-*b*-P4 VP(122K/22K) films spin coated from 0.5 wt % solution. Approximately 20 nm P4 VP cores are apparent for all block copolymer micelles micrographs because of the similar molecular weight of P4 VP blocks. Intermicelle distances for the block copolymers are approximately 40, 60, and 90 nm, respectively.

regions of the block copolymer film, both binding energies of $3d_{5/2}$ and $3d_{3/2}$ of the pristine Ag NPs at 368.8 and 375 eV, respectively without DT-Au NPs were shifted to the lower energy of approximately 0.5 eV. The results indicate that the long-range dipolar interaction indeed occurred between Ag and Au NPs in the micelle film. The interaction of the two nanoparticles in the PS-*b*-P4 VP-(47K/21K) micelles was also evidenced by the XPS spectra of DT-Au NPs in Figure 6b in which the two characteristic $4f_{7/2}$ and $4f_{5/2}$ peaks from Au NPs appearing at 84.1 and 87.8 eV, respectively, without Ag NPs were shifted to the higher energy of approximately 0.4 eV in the presence of Ag NPs in the cores. The change of the characteristic binding energies of Ag and Au NPs to the higher and lower energy levels is attributed to the relative charging and discharging of electrons on the surface of Ag and Au NPs, respectively. In fact, it has been known that the surface of Ag NPs is readily charged by the electrons from Au nanoparticles protected with the electron rich functional groups.[43,44] The excess electrons in the dodecanethiol groups covering Au NPs may be excited upon thermal annealing and transferred to the relatively electron attracting vinylpyridine groups in P4 VP, resulting in charging the surface of Ag NPs in the P4 VP cores.

To further confirm the role of block copolymer template in the composites, we additionally employed two other PS-*b*-P4 VP copolymers: PS-*b*-P4 VP(19K/22K) and PS-*b*-P4 VP(122K/22K), which had different PS

(43) Qiu, L.; Liu, F.; Zhao, L.; Wang, W.; Yao, J. *Langmuir* **2006**, *22*, 4480.
(44) Li, J.; Guo, L.; Zhang, L.; Yu, C.; Yu, L.; Jiang, P.; Wei, C.; Qin, F.; Shi, J. *Dalton Trans.* **2009**, 823.

molecular weights with P4 VP block remaining almost the same length as PS-*b*-P4 VP(47K/21K). The three different micelles formed in toluene are supposed to have the similar P4 VP cores but different PS coronas in size as shown in schematic of Figure 7 and in turn to allow us to control the average interparticle distance of Ag and DT-Au NPs in the films. UV−vis spectra obtained from the thin composite films of the three PS-*b*-P4 VP copolymers with Ag and DT-Au NPs clearly indicate that the maximum peak position of the coupled SPB is red-shifted with the increase of the interparticle distance as shown in Figure 7a. The average micelle-to-micelle distances of the three block copolymers were obtained from TEM micrographs in Figure 7b−d of thin spin coated films and turned out approximately 40, 60, and 90 nm for PS-*b*-P4 VP(19K/22K), PS-*b*-P4 VP(47K/21K) and PS-*b*-P4 VP(122K/22K), respectively. Large spacial fluctuation of long PS chains in PS-*b*-P4 VP(47K/21K) and PS-*b*-P4 VP(122K/22K) results in the PS coronas more varied in thickness than PS-*b*-P4 VP(19K/22K). The more distributed interparticle distance of Ag and DT-Au NPs located in core and corona regions, respectively gives rise to the less interparticle coupling and red-shifted spectra as shown in Figure 7a.

Conclusions

The selective deposition of Ag and DT-Au NPs in the core and corona regions of a PS-*b*-P4 VP micelle thin film, respectively, gave rise to the effective SPB coupling of the two nanoparticles. The variation of DT-Au NPs in the composites allowed the broad range control of the coupled SPB over 100 nm in wavelength. Self-assembled block copolymer micelles offer a useful template for selective loading of different metal NPs, allowing a thin uniform and homogeneous film with the capability of tailoring surface plasmon resonance band.

Acknowledgment. This project was supported by DAPA and ADD, the Korea Science and Engineering Foundation (KOSEF) grant funded by the Korea government (MOST) (R11-2007-050-03001-0), and "SYSTEM2010" project sponsored by Korea Commerce, Industry and Energy and Seoul Research and Business Development Program (10701).

Supporting Information Available: Three additional figures (PDF). This material is available free of charge via the Internet at http://pubs.acs.org.